

Warner

CILIARY INTER-MICROTUBULE BRIDGES

F. D. WARNER

*Department of Biology, Biological Research Laboratories,
Syracuse University, Syracuse, New York 13210, U.S.A.*

SUMMARY

Electron micrographs of both negatively contrasted and thin-sectioned lamellibranch gill cilia reveal several new features of ciliary fine structure, particularly in regard to those structures forming intermittent or permanent crossbridges between microtubules. Negative-contrast reveals the presence of a 14.5-nm repeating bridge between the central microtubules. Frontal views of negatively contrasted dynein arm rows along subfibre A show that the 24-nm repeat) in the outer row are displaced in a left-handed manner by 3-4 nm with respect to those in the inner row. This displacement is probably a direct reflexion of the helical subunit lattice of the subfibre. Interdoublet (nexin) links are seen connecting adjacent A and B subfibres at intervals of 86 nm along the doublet. Negative-contrast shows thin, elastic connexions holding the doublets together. When seen in longitudinal thin sections, the interdoublet links are often tilted to considerable angles, indicating they may have a specific response to interdoublet sliding.

INTRODUCTION

The motile 9+2 axoneme of cilia, flagella and sperm tails is an interconnected network of microtubules having no fewer than 5 kinds of structures forming either intermittent or permanent crossbridges between microtubules (see Warner, 1974, for review). Studies by Summers & Gibbons (1971, 1973) and Gibbons & Gibbons (1972, 1973) have clearly shown that the generative force for flagellar motility results from ATP hydrolysis) crossbridge formation between adjacent doublet microtubules. This mechanochemical interaction results in sliding displacement between the microtubules which is simultaneously converted into propagated bending motion. Recently, we examined the role of the radial spokes in the sliding-bending conversion (Warner & Satir, 1974) and concluded that the spokes, in lamellibranch gill cilia, are the primary source of the internal shear resistance required to convert active microtubule sliding into regulated, propagated bending of the organelle. Although the study presented many new details of ciliary fine structure, the observations were primarily limited to the radial spoke-central sheath complex. Using both thin-sectioned and negatively contrasted, isolated gill cilia, it is now possible to visualize the presence of a bridge between the 2 central microtubules, to determine the organization of the interdoublet or nexin links and to characterize the organization of the 2 rows of dynein arms along the doublet subfibre A.

alone
IPC
shate
plus

MATERIALS AND METHODS

Lamellibranch gill cilia from the genus *Umbonychia* were used in this study. For electron microscopy, gill tissue was isolated and fixed in 2% glutaraldehyde adjusted to pH 7.4 with 25 mM sodium cacodylate for 1.5 h at 4 °C. Tissue was postfixed in cacodylate-buffered 1% OsO₄ for 45 min, dehydrated in an ethanol series and embedded in Epon 812. Thin sections were stained for 15 min in 5% aqueous uranyl acetate followed by staining for 2 min in Reynolds' lead citrate.

For some preparations, gill tissue was deciliated and the cilia purified by differential centrifugation. Purified cilia were demembrated in Triton X-100 and either fixed as above or negatively contrasted with 2% aqueous uranyl acetate at pH 4.5. Isolated axonemes are functionally intact; that is, they will reactivate and beat normally upon the addition of ATP. Details of the isolation, purification and reactivation procedure will be published in a future paper.

OBSERVATIONS AND DISCUSSION

The movement of axonemal microtubules during ciliary or flagellar beating may be regarded as a very dynamic process, since each doublet microtubule slides with respect to every other doublet and with respect to the central microtubule complex. Even though the major part of this sliding may be only a passive response to the sliding generated between any 2 doublets at a particular instant during the beat cycle. Since we know that each linear element moves with respect to all other linear elements (Warner, 1972; Warner & Satir, 1974), all structural crossbridges between microtubules, whether intermittent or permanent, must be brought into the conceptual framework of the sliding filament model of ciliary motility (Satir, 1968).

Central microtubule bridge

Lamellibranch gill cilia have a prominent 'bridge' which occurs between doublets 5 and 6 and forms the main morphological marker for determining orientation of the cilium (Gibbons, 1961; Satir, 1965, 1968). The bridge appears to be a manifestation of arm structure between these doublets, that is, the arms of doublet 5 appear to be permanently crossbridged to doublet 6. The bridge is readily apparent in transversely sectioned cilia (Figs. 1, 11-14) and individual elements repeat at 23 nm along the A subfibre (Warner & Satir, 1974).

Our previous study of lamellibranch gill cilia (Warner & Satir, 1974) described in detail the organization of the central sheath-microtubule complex. The sheath consists of paired rows of projections along each of the 2 central microtubules to which are attached, intermittently, the radial spoke heads. Longitudinal thin sections suggest the presence of a periodic bridge between the central tubules (as have numerous other studies, e.g. Gibbons, 1961) but superimposition of the sheath projection rows also account for the bridged appearance, particularly since the measured periodicity is the same for both projections and the bridge region.

When seen in transverse sections, the central sheath projections, although not clearly resolved, form a circular profile around the central tubules (Fig. 1) and the bridge also appears to be material or a bridge joining the 2 tubules at the axoneme axis. The bridge spans the 8-nm space between tubules and often appears to be double-

over, a straightforward interpretation is provided by negative staining.

Fig. 2 shows an example which separates the images of the central pair with respect to the angle of doublet rotation. The central pair with respect to a single doublet remains in the same relative position with respect to a 4.5-nm repeating unit, except that the center of rotation is only one of the doublets in a single row of bridge material. This applies to positions

Main arm organization

All motile 9+2 cilia show orderly rows of microtubules in the principal plane. The results in doublet motility was beating of a doublet, that the control film of the precise or remained an brush between doublets, usually a doublet to suggest to other row lines, both negative, even individual negative elements repeat of superimposed, and to relationships, from doublet (Figs. 7) of negatively. Two row of the central plane (Fig. 1) and the bridge material

ed in this study. For electron micrographs, the pH was adjusted to pH 7.4 with 25 mM cacodylate-buffered 1% OsO₄ in Epon 812. Thin sections were stained for 2 min in Reynolds' lead citrate.

The cilia purified by differential centrifugation were fixed with OsO₄ in cacodylate buffer at pH 4.5. Isolated axonemes are normally upon the addition of ATP. The procedure will be published in a future issue.

The ciliary or flagellar beating microtubule doublet slides with the central microtubule complex give a passive response to the active flagellar instant during the beat cycle. In respect to all other linear elements, the central crossbridges between microtubules be brought into the conceptual framework (Satir, 1968).

which occurs between doublet microtubules is a marker for determining orientation (Satir, 1968). The bridge appears to be double, that is, the arms of both rows are attached to doublet 6. The bridge is composed of 11-14) and individual elements (Satir, 1974).

Merz & Satir, 1974) described the central microtubule complex. The sheath complex connects the central microtubules to which are attached in longitudinal thin sections suggested that the central microtubules (as have numerous other microtubules) the sheath projection rows could be the measured periodicity is 23 nm.

The sheath projections, although not attached to the central tubules (Fig. 1) and their periodicity at the axoneme axis. This periodicity appears to be double. How-

ever, a straightforward answer regarding the presence of a central microtubule bridge is provided by negatively contrasted images of the central complex.

Fig. 2 shows an intact central tubule-sheath complex and again it is not possible to separate the image of the sheath projections from the bridge region. Fig. 3 shows a central pair with most of the sheath material solubilized except that along 1 tubule, a single doublet remains attached to the sheath via the triplet radial spokes. Fig. 4 shows a central pair with all sheath material removed: clearly there remains a prominent 23-nm repeating bridge between the 2 tubules. Fig. 5 shows a similar preparation except that the central pair has pulled apart and the bridge elements remain attached to only one of the tubules. Although it appears from these preparations that only a single row of bridge elements occurs between the central tubules, the same arguments that apply to possible dynein arm superimposition (see next section) also apply here.

Dynein arm organization

All motile 9 + 2 cilia, flagella and spermtails have an ATPase, dynein, located in the orderly rows of arms of subfibre A of each doublet microtubule. The dynein arms are the principal and probably sole source of mechanochemical interaction which results in doublet sliding (Summers & Gibbons, 1971, 1973). This mechanochemical activity was beautifully demonstrated by Gibbons & Gibbons (1973) when they selectively solubilized only the 9 outer rows of arms and observed, in ATP-reactivated flagella, that the axonemes then beat with precisely one-half the frequency of untreated control flagella.

The precise organization and periodicity of the dynein arms along a given doublet has remained uncertain, mainly because it is difficult both to preserve and to distinguish between the 2 rows when seen in longitudinal thin sections, and negative-contrast usually results in their solubilization. The reported periodicity of arms along a doublet spans a considerable range (12-24 nm), which has caused Chasey (1972) to suggest that the arms of 1 row may be half-staggered with respect to those of the other row. Thus the 12-24 nm range could be easily accounted for, if in some instances both rows had been seen superimposed while in other instances they had been seen individually.

Both negatively contrasted and thin-sectioned arm rows are seen in Figs. 6 and 15. The arms repeat at 23 nm, centre-to-centre along the subfibre. Although the possibility of superimposition of the 2 adjacent rows cannot be ruled out in images such as Fig. 6, it appears that only a single row is represented. To test for superimposition artifact, and to provide a straightforward answer as to arm period and inter-row relationships, frontal views of the arms are required; that is, both rows of arms along a single doublet subfibre A need to be viewed from the position of the opposing B subfibre. Figs. 7 and 8 show frontal views of the dynein arm rows from doublets at the edges of negatively contrasted, demembrated but structurally intact cilia similar to Fig. 6. Two rows can be seen along each doublet and the arm periodicity in each row is 23 nm centre-to-centre. Occasionally the arm rows have an obvious scalloped appearance (Fig. 9), which probably results from overlying regions of incompletely solubilized membrane. It is apparent in Figs. 7 and 8 that the 2 rows are slightly

displaced, that is, the arms in one row are not in lateral register with those of the other row. Although precise measurement is difficult, the arms in the outer row appear to be displaced in a left-handed manner by 3–4 nm (10 degrees) with respect to their immediate neighbour in the inner row. The 2 rows are separated by 15–16 nm. This displacement is consistent with the helical displacement of tubulin subunits found in the subfibre by Amos & Klug (1974). It is reasonable to think that the arms are precisely positioned on the A subfibre with respect to one of the helical families of the tubulin subunit lattice. The observed arm displacement matches most favourably with the start, left-handed family, assuming that 2–3 protofilaments lie between the 2 rows of arms. However, optical diffraction data are necessary to match precisely the arm arrangement with the tubulin helix.

The high frequency of appearance of the double rows of arms (sometimes seen on both sides of the same axoneme) eliminates the possibility of the image representing only the doublets 5–6 bridge. Although usually the arms are not visible on fragmented doublet microtubules, occasionally a prominent 23-nm repeat can be seen which is probably related to one of the rows (Fig. 10).

Interdoublet link organization

Thin connexions, termed interdoublet, nexin or circumferential links (for review see Stephens, 1974; Warner, 1974) are often seen in cross-sections of ciliary flagella. The links lie near the centrifugal side of the inner dynein arms and extend about 18 nm to the adjacent B subfibre (Figs. 11–14). The visibility of the links is enhanced in demembranated axonemes, presumably because of the loss of a structural matrix material from the organelle (e.g. compare Figs. 11 and 12). The frequency of appearance of the links in a given ciliary cross-section is low (~2; Figs. 11, 13; Fig. 12 is exceptional), suggesting that their periodicity along the doublet is in the range of typical section thickness (70–100 nm). The inter-doublet link should not be confused with similar but structurally prominent connexions between doublet microtubules that are restricted to the region immediately distal to the basal plate of some cilia and flagella (e.g., *Chlamydomonas* flagella; Witman, Carlsson, Berliner & Rosenbaum, 1972).

Stephens (1970) attempted an initial characterization of the interdoublet link material in *Arbacia* sperm flagella and termed the isolated protein nexin. His thin-layer fractionated preparations consisted largely of A subfibres to which adhered clumped material repeating at about 100 nm along the subfibre. When negatively stained, the clumped material seemed to hold adjacent A subfibres together on the carbon supporting film, and Stephens concluded that the material, nexin, joined adjacent A subfibres in the native organelle, rather than joining A to B. Similar interpretations have been made on sectioned cilia (Linck, 1973*a, b*) although the published micrographs generally do not substantiate that conclusion.

In the present study, cross-sections of isolated, demembranated cilia indicate that the interdoublet link joins A subfibres to adjacent B subfibres, and similar links appear in numerous other studies (e.g. Gibbons & Fronk, 1972; Gibbons & Gibbons, 1973; Linck, 1973*a, b*). Furthermore, when the links are occasionally seen

in longitudinal sections (Fig. 15) the conflict between Stephens' interpretation and species differences seem unlikely. The grouping along the A subfibre clearly reveal the 86-nm repeat of the A subfibre (Fig. 16). The carbon supporting film, which is of low affinity (probably artificial), does not appear to be a major axonemal component.

At the time of Stephens' work, nexin links were a major axonemal component. They were seen as distinct groups of clumped material between adjacent doublet microtubule nexin links (Stephens, 1970) and do not resemble the thin layer fractionated material. Negatively contrasted gels of doublets of adjacent doublet microtubules show a similar periodicity, but the smaller repeat is about 100 nm. It is obvious that in preparations the links may be broken. Connections were seen by Linck (1973*a*). However, it should be cautioned that the material is not unequivocally identified as nexin.

Recently, Dallai, Berni & Berti (1973) in cross-sections of *Sciara* sperm flagella, the links are seen to be similar to that occurring in cilia. They appear as a thin coating between adjacent doublets. These links are not restricted to doublets. It represents a circumferential link between adjacent doublets.

Although the interdoublet link is a regular, typically repeating component, it is only visible in cross-sections of the inner and outer rows of doublets. The A subfibre (see below) is a regular component. Stephens' discussions of nexin are consistent with that, like any other protein, in some manner it is involved in the mechanism for the assembly of the microtubule. The links are inherent to the doublet, and must be present in all doublets. No

ral register with those of the arms in the outer row appear to differ (degrees) with respect to their orientation by 15–16 nm. This displacement of tubulin subunits found in the arms leads me to think that the arms are produced by the helical families of the tubulin. The arms match most favourably with the nexin link segments lie between the 2 arms and the nexin link to match precisely the arms.

rows of arms (sometimes seen in cross-sections) the visibility of the image representation of the arms are not visible on fragments of the nexin link. A 15–16 nm repeat can be seen when the arms are seen in cross-sections.

circumferential links (for example, in cross-sections of cilia and flagella) between the inner dynein arms and external microtubules (Fig. 14). The visibility of the links is often obscured, probably because of the loss of contrast in the micrographs (compare Figs. 11 and 12). The contrast in every cross-section is low (< 20% of the contrast of their periodicity along the doublet, 86 nm). The inter-doublet links are the most prominent connexions between adjacent doublets immediately distal to the basal body (Linck, 1973; *Sciara* flagella; Witman, Carlsson & Warner, 1974).

Warner's (1974) interpretation of the interdoublet links is that they are made of a protein nexin. His thermal denaturation studies refer to which adhered clumps of nexin were destroyed. When negatively stained, the nexin links are seen together on the carbon support film. The nexin, joined adjacent A and B subfibres, joined adjacent A and B. Similar interpretations have been made from the published micrographs of the interdoublet links.

Warner's (1974) interpretation of the interdoublet links is that they are made of a protein nexin. His thermal denaturation studies refer to which adhered clumps of nexin were destroyed. When negatively stained, the nexin links are seen together on the carbon support film. The nexin, joined adjacent A and B subfibres, joined adjacent A and B. Similar interpretations have been made from the published micrographs of the interdoublet links.

In longitudinal sections (Fig. 15), they still appear to join A to B. The apparent discrepancy between Stephens' (1970, 1971, 1974) observations and the present study (the differences seem unlikely) can probably be resolved by analysis of radial spoke groups along the A subfibre. Negatively contrasted preparations of collapsed gill cilia reveal the 86-nm repeat triplet grouping of the radial spokes (Figs. 3, 16). The spokes, however, are often collapsed together into repeating clumps of material along the A subfibre (Fig. 16). The spokes appear to hold the doublets firmly together on the supporting film, which suggests that the spoke material is 'sticky' and has a high affinity (probably artifactual) for other axoneme components or microtubules. At the time of Stephens' (1970) study, it was not generally known that the radial spokes were a major axonemal component and it is possible that the nexin links were made up of groups of clumped radial spokes. His micrographs of negatively contrasted A subfibres and nexin links (Stephens, 1971) strongly resemble the spoke groups in Fig. 16, but do not resemble the thin connexions observed in this study (see below).

Negatively contrasted gill cilia occasionally show thin connexions joining the A and B subfibres of adjacent doublets (Fig. 17). These thin links are somewhat irregular in width, but the smallest separation measured is about 50 nm, while the largest is about 100 nm. It is obvious that the connexion has stretched considerably and in some instances the links may span as much as 300 nm between doublets. Similar connexions were seen by Linck (1973b) in negatively contrasted *Aequipecten* gill cilia. However, it should be cautioned that the thin connexions visible in Fig. 17 cannot be unequivocally identified as the interdoublet links appearing in thin sections (Figs. 14, 15).

Recently, Dallai, Bernini & Giusti (1973) described interdoublet connexions in the flagella of *Sciara* sperm flagella, which do not have the usual 9+2 organization. In cross-sections, the links clearly join adjacent A and B doublet subfibres in a position similar to that occurring in 9+2 cilia and flagella. When negatively contrasted, the links appear as a thin connexion between subfibres with a regular repeat of about 86 nm. These links are also very elastic, often spanning 200–300 nm separations between doublets. It remains to be determined if these connexions are homologous to the interdoublet links of 9+2 axonemes.

When the interdoublet links are seen in longitudinal thin sections, their periodicity is regular, typically lying at about 86-nm intervals along the doublet (Fig. 15). The links are only visible in the region where the section plane appears to pass between the inner and outer rows of dynein arms and they usually lie at angles other than 90° to the A subfibre (see below).

Previous discussions of the interdoublet links (Warner, 1974; Warner & Satir, 1974) have suggested that, like any connexions between sliding microtubules, the links must be capable of some manner of displacement in order to permit interdoublet sliding. Two possible mechanisms for this displacement exist: (1) the links function as part of a mechanochemical event, perhaps interacting with the inner row of dynein arms; or (2) the links are inherently elastic and thus capable of considerable angular displacement, which must be at least as great as the maximum relative movement between adjacent doublets. No evidence exists in support of the first contention and little can

be said except that mechanochemical activity of these structures would substantially increase the complexity and coordination of known mechanochemical events related to the sliding-bending mechanism.

Certain evidence supports the idea that the links may be inherently elastic, apart from the observation of extensive stretching of intermicrotubule connexions in negatively contrasted preparations (Fig. 17; Dallai *et al.* 1973; Linck, 1973*b*). Fig. 15 shows several interdoublet links in longitudinal section of a cilium. The links are uniformly tilted to an angle of about 45° from the perpendicular. Since the normal (interdoublet sliding absent) orientation of the links appears to be perpendicular to the doublet, it appears that some interdoublet displacement and concomitant link extension is visible in this particular cilium. Knowing the distance separating adjacent A and B subfibres (18 nm) and the link angle (45°), it is possible to calculate from simple geometrical expressions (Warner, 1972; Warner & Satir, 1974), both the amount of interdoublet sliding that has occurred and the necessary link extension to accommodate this sliding. For Fig. 15, the displacement is about 18 nm, requiring a total link length of about 25.5 nm, which is an approximate 41% increase. Maximum predicted interdoublet sliding (doublets 3-4, 7-8) is about 30 nm for a cilium with a bend angle of 100° , requiring an approximate 90% increase in the length and a maximum bend angle of 60° of the interdoublet connexions. Several images similar to Fig. 15 have been obtained with maximum link angles of about 55° , which strongly supports the notion that the links are permanently bridged and inherently elastic and thus capable of significant angular displacement in response to interdoublet sliding.

The function of the interdoublet links in the motile mechanism must, for the time being, remain speculative. Are they an elastic force providing shear resistance and related directly to the sliding-bending conversion, or do they simply represent a component which contributes to the maintenance of geometrical positioning within the axoneme? Summers & Gibbons (1971, 1973) briefly treated isolated sperm flagella with trypsin, resulting in partial proteolytic disruption of both the interdoublet links and the radial spokes. The flagella then lost the capacity to beat normally upon addition of ATP but retained the capacity for active interdoublet sliding. Similar results have been obtained with isolated gill cilia (Warner, unpublished results). Clearly then, one or both of these linkage components function during bending. Although data from Warner & Satir (1974) indicate that radial spoke activity is the primary event associated with the conversion of active sliding into regular bending.

This study was supported by research grants GB 41552 from the National Science Foundation and GM 20690 from the National Institutes of Health. It is a pleasure to thank Ms. C. Perkins for expert technical assistance.

REFERENCES

- AMOS, L. A. & KLUG, A. (1972). *J. Cell Biol.* **14**, 523-549.
- CRANEY, D. (1972). *J. Cell Biol.* **74**, 471-479.
- DALLAI, R., BERNINI, F. & LINCK, R. W. (1973). The complex of *Sciara*. *J. Cell Biol.* **35**, 1-10.
- GIBBONS, B. H. & GIBBONS, R. E. (1971). Activity in sea urchin sperm flagella. *J. Cell Biol.* **14**, 1-10.
- GIBBONS, B. H. & GIBBONS, R. E. (1973). Movement of reactive sites in sea urchin sperm flagella. *J. Cell Biol.* **14**, 1-10.
- GIBBONS, I. R. (1961). The structure of the lamellibranch sperm flagellum. *J. Cell Biol.* **1**, 1-10.
- GIBBONS, I. R. & FROST, J. (1968). The sperm flagellum of the mollusc, *Aequipecten irradians*. *J. Cell Biol.* **1**, 1-10.
- LINCK, R. W. (1973*a*). The structure of the mollusc, *Aequipecten irradians*. *J. Cell Biol.* **1**, 1-10.
- LINCK, R. W. (1973*b*). The structure of the mollusc, *Aequipecten irradians*. *J. Cell Biol.* **1**, 1-10.
- SUMMERS, P. (1965). Studies on the filamentous structure of the flagellum of the mollusc, *Aequipecten irradians*. *J. Cell Biol.* **1**, 1-10.
- SUMMERS, P. (1968). Studies on the filamentous structure of the flagellum of the mollusc, *Aequipecten irradians*. *J. Cell Biol.* **1**, 1-10.
- SUMMERS, R. E. (1970). The structure of the nine-fold coil of the sperm flagellum of the mollusc, *Aequipecten irradians*. *J. Cell Biol.* **1**, 1-10.
- SUMMERS, R. E. (1971). The structure of the nine-fold coil of the sperm flagellum of the mollusc, *Aequipecten irradians*. *J. Cell Biol.* **1**, 1-10.
- SUMMERS, R. E. (1973). The structure of the nine-fold coil of the sperm flagellum of the mollusc, *Aequipecten irradians*. *J. Cell Biol.* **1**, 1-10.
- SUMMERS, R. E. (1974). The structure of the nine-fold coil of the sperm flagellum of the mollusc, *Aequipecten irradians*. *J. Cell Biol.* **1**, 1-10.
- SUMMERS, R. E. (1975). The structure of the nine-fold coil of the sperm flagellum of the mollusc, *Aequipecten irradians*. *J. Cell Biol.* **1**, 1-10.
- SUMMERS, R. E. (1976). The structure of the nine-fold coil of the sperm flagellum of the mollusc, *Aequipecten irradians*. *J. Cell Biol.* **1**, 1-10.
- SUMMERS, R. E. (1977). The structure of the nine-fold coil of the sperm flagellum of the mollusc, *Aequipecten irradians*. *J. Cell Biol.* **1**, 1-10.
- SUMMERS, R. E. (1978). The structure of the nine-fold coil of the sperm flagellum of the mollusc, *Aequipecten irradians*. *J. Cell Biol.* **1**, 1-10.
- SUMMERS, R. E. (1979). The structure of the nine-fold coil of the sperm flagellum of the mollusc, *Aequipecten irradians*. *J. Cell Biol.* **1**, 1-10.
- SUMMERS, R. E. (1980). The structure of the nine-fold coil of the sperm flagellum of the mollusc, *Aequipecten irradians*. *J. Cell Biol.* **1**, 1-10.
- SUMMERS, R. E. (1981). The structure of the nine-fold coil of the sperm flagellum of the mollusc, *Aequipecten irradians*. *J. Cell Biol.* **1**, 1-10.
- SUMMERS, R. E. (1982). The structure of the nine-fold coil of the sperm flagellum of the mollusc, *Aequipecten irradians*. *J. Cell Biol.* **1**, 1-10.
- SUMMERS, R. E. (1983). The structure of the nine-fold coil of the sperm flagellum of the mollusc, *Aequipecten irradians*. *J. Cell Biol.* **1**, 1-10.
- SUMMERS, R. E. (1984). The structure of the nine-fold coil of the sperm flagellum of the mollusc, *Aequipecten irradians*. *J. Cell Biol.* **1**, 1-10.
- SUMMERS, R. E. (1985). The structure of the nine-fold coil of the sperm flagellum of the mollusc, *Aequipecten irradians*. *J. Cell Biol.* **1**, 1-10.
- SUMMERS, R. E. (1986). The structure of the nine-fold coil of the sperm flagellum of the mollusc, *Aequipecten irradians*. *J. Cell Biol.* **1**, 1-10.
- SUMMERS, R. E. (1987). The structure of the nine-fold coil of the sperm flagellum of the mollusc, *Aequipecten irradians*. *J. Cell Biol.* **1**, 1-10.
- SUMMERS, R. E. (1988). The structure of the nine-fold coil of the sperm flagellum of the mollusc, *Aequipecten irradians*. *J. Cell Biol.* **1**, 1-10.
- SUMMERS, R. E. (1989). The structure of the nine-fold coil of the sperm flagellum of the mollusc, *Aequipecten irradians*. *J. Cell Biol.* **1**, 1-10.
- SUMMERS, R. E. (1990). The structure of the nine-fold coil of the sperm flagellum of the mollusc, *Aequipecten irradians*. *J. Cell Biol.* **1**, 1-10.
- SUMMERS, R. E. (1991). The structure of the nine-fold coil of the sperm flagellum of the mollusc, *Aequipecten irradians*. *J. Cell Biol.* **1**, 1-10.
- SUMMERS, R. E. (1992). The structure of the nine-fold coil of the sperm flagellum of the mollusc, *Aequipecten irradians*. *J. Cell Biol.* **1**, 1-10.
- SUMMERS, R. E. (1993). The structure of the nine-fold coil of the sperm flagellum of the mollusc, *Aequipecten irradians*. *J. Cell Biol.* **1**, 1-10.
- SUMMERS, R. E. (1994). The structure of the nine-fold coil of the sperm flagellum of the mollusc, *Aequipecten irradians*. *J. Cell Biol.* **1**, 1-10.
- SUMMERS, R. E. (1995). The structure of the nine-fold coil of the sperm flagellum of the mollusc, *Aequipecten irradians*. *J. Cell Biol.* **1**, 1-10.
- SUMMERS, R. E. (1996). The structure of the nine-fold coil of the sperm flagellum of the mollusc, *Aequipecten irradians*. *J. Cell Biol.* **1**, 1-10.
- SUMMERS, R. E. (1997). The structure of the nine-fold coil of the sperm flagellum of the mollusc, *Aequipecten irradians*. *J. Cell Biol.* **1**, 1-10.
- SUMMERS, R. E. (1998). The structure of the nine-fold coil of the sperm flagellum of the mollusc, *Aequipecten irradians*. *J. Cell Biol.* **1**, 1-10.
- SUMMERS, R. E. (1999). The structure of the nine-fold coil of the sperm flagellum of the mollusc, *Aequipecten irradians*. *J. Cell Biol.* **1**, 1-10.
- SUMMERS, R. E. (2000). The structure of the nine-fold coil of the sperm flagellum of the mollusc, *Aequipecten irradians*. *J. Cell Biol.* **1**, 1-10.
- SUMMERS, R. E. (2001). The structure of the nine-fold coil of the sperm flagellum of the mollusc, *Aequipecten irradians*. *J. Cell Biol.* **1**, 1-10.
- SUMMERS, R. E. (2002). The structure of the nine-fold coil of the sperm flagellum of the mollusc, *Aequipecten irradians*. *J. Cell Biol.* **1**, 1-10.
- SUMMERS, R. E. (2003). The structure of the nine-fold coil of the sperm flagellum of the mollusc, *Aequipecten irradians*. *J. Cell Biol.* **1**, 1-10.
- SUMMERS, R. E. (2004). The structure of the nine-fold coil of the sperm flagellum of the mollusc, *Aequipecten irradians*. *J. Cell Biol.* **1**, 1-10.
- SUMMERS, R. E. (2005). The structure of the nine-fold coil of the sperm flagellum of the mollusc, *Aequipecten irradians*. *J. Cell Biol.* **1**, 1-10.
- SUMMERS, R. E. (2006). The structure of the nine-fold coil of the sperm flagellum of the mollusc, *Aequipecten irradians*. *J. Cell Biol.* **1**, 1-10.
- SUMMERS, R. E. (2007). The structure of the nine-fold coil of the sperm flagellum of the mollusc, *Aequipecten irradians*. *J. Cell Biol.* **1**, 1-10.
- SUMMERS, R. E. (2008). The structure of the nine-fold coil of the sperm flagellum of the mollusc, *Aequipecten irradians*. *J. Cell Biol.* **1**, 1-10.
- SUMMERS, R. E. (2009). The structure of the nine-fold coil of the sperm flagellum of the mollusc, *Aequipecten irradians*. *J. Cell Biol.* **1**, 1-10.
- SUMMERS, R. E. (2010). The structure of the nine-fold coil of the sperm flagellum of the mollusc, *Aequipecten irradians*. *J. Cell Biol.* **1**, 1-10.
- SUMMERS, R. E. (2011). The structure of the nine-fold coil of the sperm flagellum of the mollusc, *Aequipecten irradians*. *J. Cell Biol.* **1**, 1-10.
- SUMMERS, R. E. (2012). The structure of the nine-fold coil of the sperm flagellum of the mollusc, *Aequipecten irradians*. *J. Cell Biol.* **1**, 1-10.
- SUMMERS, R. E. (2013). The structure of the nine-fold coil of the sperm flagellum of the mollusc, *Aequipecten irradians*. *J. Cell Biol.* **1**, 1-10.
- SUMMERS, R. E. (2014). The structure of the nine-fold coil of the sperm flagellum of the mollusc, *Aequipecten irradians*. *J. Cell Biol.* **1**, 1-10.
- SUMMERS, R. E. (2015). The structure of the nine-fold coil of the sperm flagellum of the mollusc, *Aequipecten irradians*. *J. Cell Biol.* **1**, 1-10.
- SUMMERS, R. E. (2016). The structure of the nine-fold coil of the sperm flagellum of the mollusc, *Aequipecten irradians*. *J. Cell Biol.* **1**, 1-10.
- SUMMERS, R. E. (2017). The structure of the nine-fold coil of the sperm flagellum of the mollusc, *Aequipecten irradians*. *J. Cell Biol.* **1**, 1-10.
- SUMMERS, R. E. (2018). The structure of the nine-fold coil of the sperm flagellum of the mollusc, *Aequipecten irradians*. *J. Cell Biol.* **1**, 1-10.
- SUMMERS, R. E. (2019). The structure of the nine-fold coil of the sperm flagellum of the mollusc, *Aequipecten irradians*. *J. Cell Biol.* **1**, 1-10.
- SUMMERS, R. E. (2020). The structure of the nine-fold coil of the sperm flagellum of the mollusc, *Aequipecten irradians*. *J. Cell Biol.* **1**, 1-10.
- SUMMERS, R. E. (2021). The structure of the nine-fold coil of the sperm flagellum of the mollusc, *Aequipecten irradians*. *J. Cell Biol.* **1**, 1-10.
- SUMMERS, R. E. (2022). The structure of the nine-fold coil of the sperm flagellum of the mollusc, *Aequipecten irradians*. *J. Cell Biol.* **1**, 1-10.
- SUMMERS, R. E. (2023). The structure of the nine-fold coil of the sperm flagellum of the mollusc, *Aequipecten irradians*. *J. Cell Biol.* **1**, 1-10.
- SUMMERS, R. E. (2024). The structure of the nine-fold coil of the sperm flagellum of the mollusc, *Aequipecten irradians*. *J. Cell Biol.* **1**, 1-10.
- SUMMERS, R. E. (2025). The structure of the nine-fold coil of the sperm flagellum of the mollusc, *Aequipecten irradians*. *J. Cell Biol.* **1**, 1-10.

these structures would substantially influence the known mechanochemical events related to

links may be inherently elastic, and the intermicrotubule connexions in the bend region of a cilium. The linkages appear to be perpendicular to the plane of movement and concomitant link extension. Since the distance separating adjacent microtubules is possible to calculate from serial electron micrographs (Warner & Satir, 1974), both the amount of necessary link extension to accommodate a 18 nm bend, requiring a total of about 41% increase. Maximum predicted extension is 18 nm for a cilium with a bend angle of 55°, which strongly supports the idea of inherently elastic and thus capable of interdoublet sliding.

The sliding mechanism must, for the cilium to provide shear resistance and to move, or do they simply represent a passive geometrical positioning without any actively treated isolated sperm flagella. The combination of both the interdoublet capacity to beat normally upon active interdoublet sliding. Serial electron micrographs (Warner, unpublished results) show that radial spoke activity is a prerequisite for active sliding into regular

from the National Science Foundation. It is a pleasure to thank Ms C.

REFERENCES

ALLEN, J. A. & KLUG, A. (1974). Arrangement of subunits in flagellar microtubules. *J. Cell Sci.* **12**, 349-360.

ALLEN, J. D. (1972). Further observations on the cilia of *Tetrahymena pyriformis*. *Exptl Cell Res.* **74**, 470-479.

ALLEN, J. D., BERNINI, F. & GIUSTI, F. (1973). Interdoublet connections in the sperm flagellar axoneme of *Sciara*. *J. submicrosc. Cytol.* **5**, 137-145.

ALLEN, J. D., BERNINI, F., H. & GIBBONS, I. R. (1972). Flagellar movement and adenosine triphosphatase activity in sea urchin sperm extracted with Triton X-100. *J. Cell Biol.* **54**, 75-97.

ALLEN, J. D., BERNINI, F. & GIBBONS, I. R. (1973). The effect of partial extraction of dynein arms on the movement of reactivated sea-urchin sperm. *J. Cell Sci.* **13**, 337-357.

ALLEN, J. D. & SATIR, P. (1961). The relationship between the fine structure and direction of beat in gill cilia of a lamellibranch mollusc. *J. biophys. biochem. Cytol.* **11**, 179-205.

ALLEN, J. D. & FRONK, E. (1972). Some properties of bound and soluble dynein from sea urchin sperm flagella. *J. Cell Biol.* **54**, 365-381.

ALLEN, J. D. & SATIR, P. (1973a). Comparative isolation of cilia and flagella from the lamellibranch mollusc, *Aequipecten irradians*. *J. Cell Sci.* **12**, 345-367.

ALLEN, J. D. & SATIR, P. (1973b). Chemical and structural differences between cilia and flagella from the lamellibranch mollusc, *Aequipecten irradians*. *J. Cell Sci.* **12**, 951-981.

ALLEN, J. D. & SATIR, P. (1965). Studies on cilia. II. Examination of the distal region of the ciliary shaft and the relationship of the filaments in motility. *J. Cell Biol.* **26**, 805-834.

ALLEN, J. D. & SATIR, P. (1968). Studies on cilia. III. Further studies on the cilium tip and a 'sliding filament' mechanism of ciliary motility. *J. Cell Biol.* **39**, 77-94.

ALLEN, J. D. & SATIR, P. (1970). Isolation of nexin - the linkage protein responsible for the maintenance of the nine-fold configuration of flagellar axonemes. *Biol. Bull. mar. biol. Lab., Woods Hole* **119**, 118-128.

ALLEN, J. D. & SATIR, P. (1971). Microtubules. In *Biological Macromolecules*, vol. 5 (ed. S. N. Timasheff & D. Fasman), pp. 355-391. New York: Marcel Dekker.

ALLEN, J. D. & SATIR, P. (1974). Enzymatic and structural proteins of the axoneme. In *Cilia and Flagella* (ed. M. A. Sleight), pp. 39-76. London: Academic Press.

ALLEN, J. D., SATIR, P., K. E. & GIBBONS, I. R. (1971). Adenosine triphosphate-induced sliding of tubules in trypsin-treated flagella of sea urchin sperm. *Proc. natn. Acad. Sci. U.S.A.* **68**, 3092-3096.

ALLEN, J. D., SATIR, P., K. E. & GIBBONS, I. R. (1973). Effects of trypsin digestion on flagellar structures and relationship to motility. *J. Cell Biol.* **58**, 618-629.

ALLEN, J. D. & SATIR, P. (1972). Macromolecular organization of eukaryotic cilia and flagella. In *Advances in Cell and Molecular Biology*, vol. 2 (ed. E. J. Du Praw), pp. 192-235. New York: Academic Press.

ALLEN, J. D. & SATIR, P. (1974). The fine structure of the ciliary and flagellar axoneme. In *Cilia and Flagella* (ed. M. A. Sleight), pp. 11-37. London: Academic Press.

ALLEN, J. D. & SATIR, P. (1974). The structural basis of ciliary bend formation. Radial spoke structural changes accompanying microtubule sliding. *J. Cell Biol.* **63**, 35-63.

ALLEN, J. D., SATIR, P., G. B., CARLSON, K., BERLINER, J. & ROSENBAUM, J. L. (1972). *Chlamydomonas reinhardtii*. Isolation and electrophoretic analysis of microtubules, matrix, membranes, and axonemes. *J. Cell Biol.* **54**, 507-539.

(Received 22 May 1975)

All figures (except Fig. 15) are at a magnification of $\times 180000$.

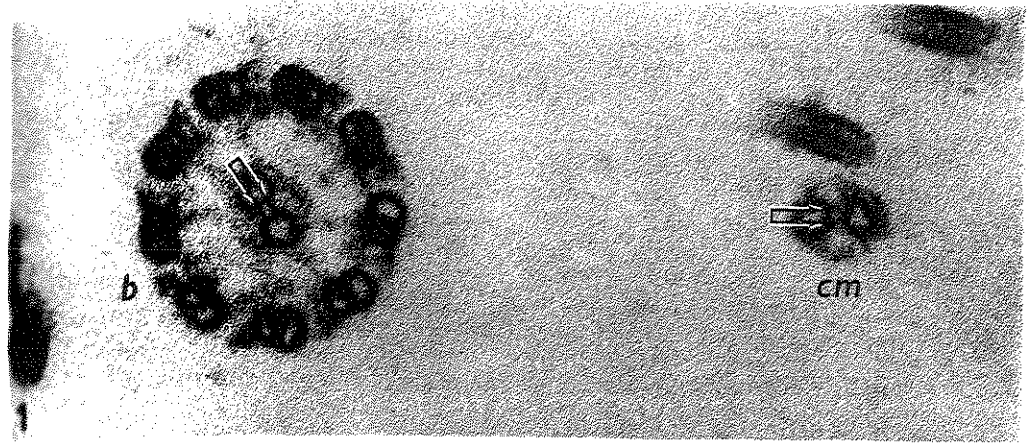
Fig. 1. Transverse section of an isolated, demembrated cilium showing an apparent bridge between the 2 central microtubules (arrows). The central tubule-sheath complex on the right (*cm*) has become separated from the remainder of the axoneme. *b*, doublets 5-6 bridge.

Fig. 2. Uranyl acetate negatively contrasted central microtubule-sheath complex. The overlying sheath projections obscure the bridge region between the 2 tubules.

Fig. 3. Central microtubule-sheath complex (*cm*) to which a single doublet (*a*, *b*) remains attached via the 86-nm repeating groups of triplet radial spokes (brackets). Most of the sheath projections have been solubilized, but because of the plane of tubule collapse, the bridge region is not clear.

Fig. 4. Central pair microtubules from which all sheath material has been solubilized. The 2 tubules remain held together by the bridge projections repeating at 14.5 nm (arrows).

Fig. 5. Central pair microtubules from which all sheath material has been solubilized. The 2 microtubules have separated but the bridge projections remain attached to one of the tubules (arrows).



nification of $\times 180000$.
nated cilium showing an apparent
. The central tubule-sheath com-
the remainder of the axoneme. *b*,
microtubule-sheath complex. The
tion between the 2 tubules.
o which a single doublet (*a*, *b*) re-
f triplet radial spokes (brackets).
zed, but because of the plane of
eath material has been solubilized.
projections repeating at 14.5 nm
eath material has been solubilized.
projections remain attached to one

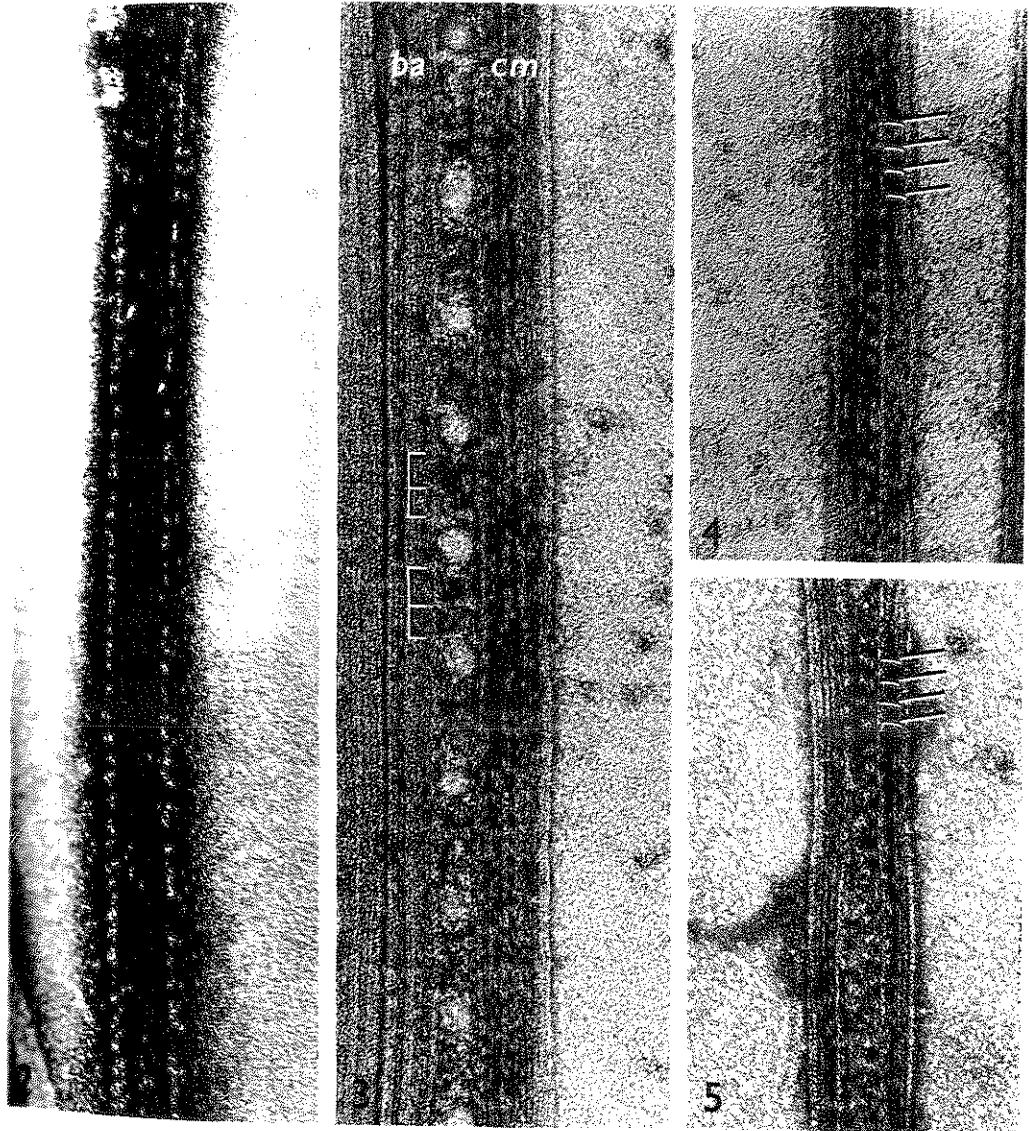
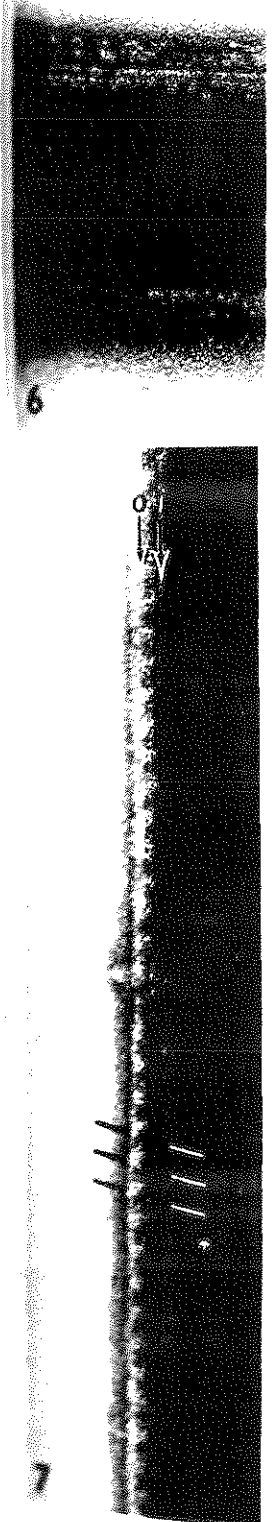


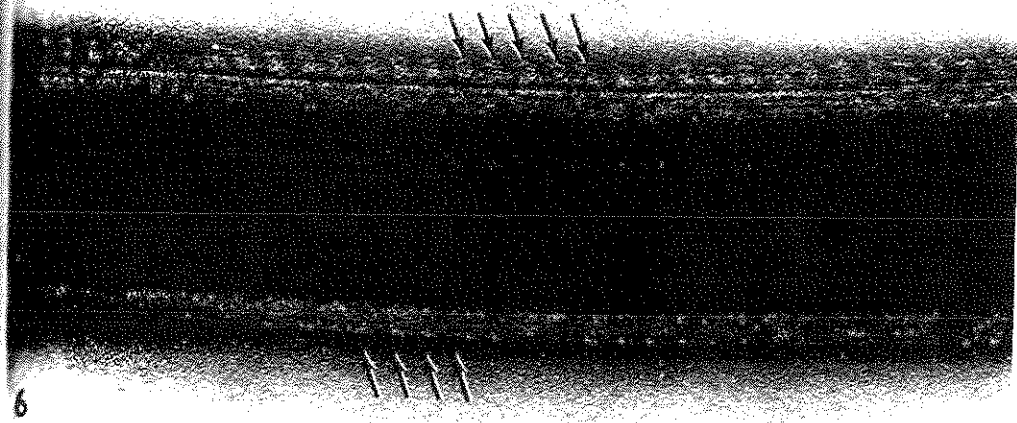
Fig. 6. Uranyl acetate negatively contrasted, intact but demembrated cilium. Single rows of dynein arms repeating at 23 nm are visible at both sides of the axoneme (arrows).

Figs. 7, 8. Frontal views of subfibre A from a doublet at the edge of an intact cilium. Both the inner (*i*) and outer (*o*) arm rows are visible: the arms repeat at 23 nm in both rows. Arms of the outer row appear to be displaced by 3-4 nm in a left-handed manner with respect to the arms in the inner row (lines).

Fig. 9. Frontal view of a doublet where it appears that incompletely solubilized membrane has collapsed over the arm rows resulting in a characteristic scalloped appearance (arrows). The scallop repeat is 23 nm.

Fig. 10. Fragmented doublet microtubule showing a prominent 23-nm repeat (arrows) that is probably related to one of the arm rows. The repeat appears to be contrasted in the cleft between the 2 subfibres of the doublet.





demembrated cilium. Single
at both sides of the axoneme

at the edge of an intact cilium.
the arms repeat at 23 nm in both
by 3-4 nm in a left-handed
twist).

incompletely solubilized mem-
ber characteristic scalloped appear-

prominent 23-nm repeat (arrows)
repeat appears to be contrasted in

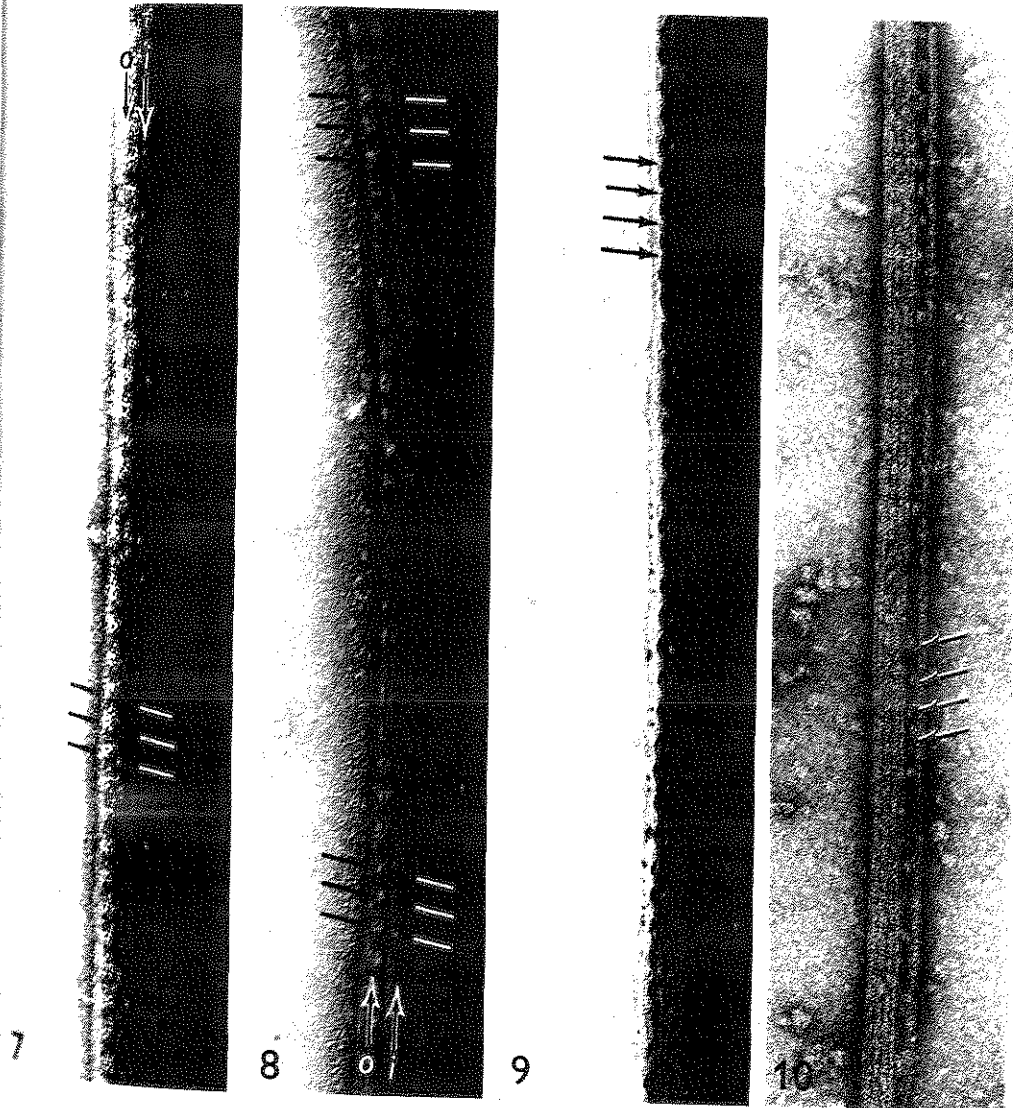
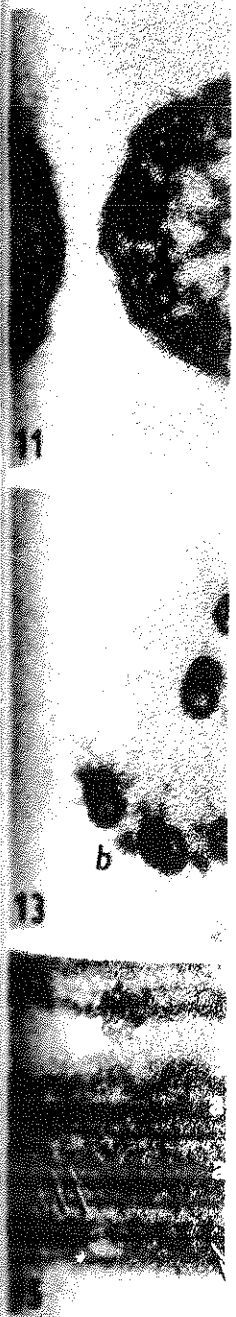


Fig. 11. *In situ* cilium seen in transverse section. Interdoublet links (arrows) connect adjacent A and B subfibres in the region of the inner dynein arms. The direction of view is from cilium base-to-tip with the doublets 5-6 bridge (*b*) located in the 6 o'clock position.

Figs. 12-14. Isolated, demembranated cilia seen in varying degrees of disassociation. Interdoublet links can be seen in all cilia but are particularly clear in Fig. 12. Cilium orientation and bridge (*b*) position is the same as in Fig. 11.

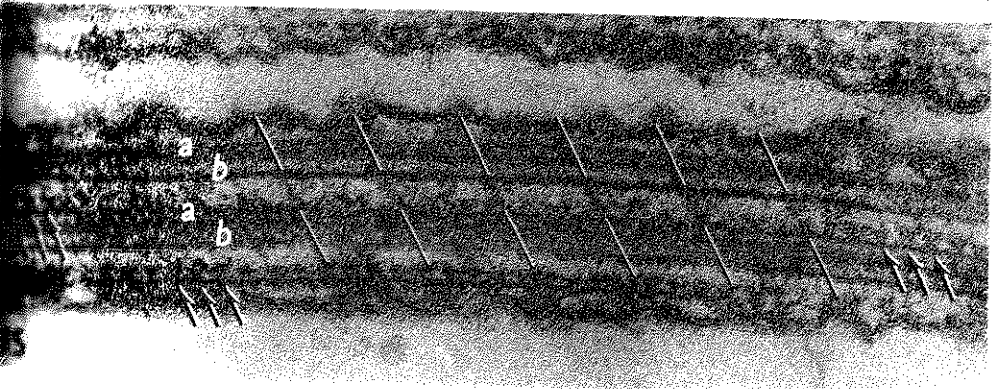
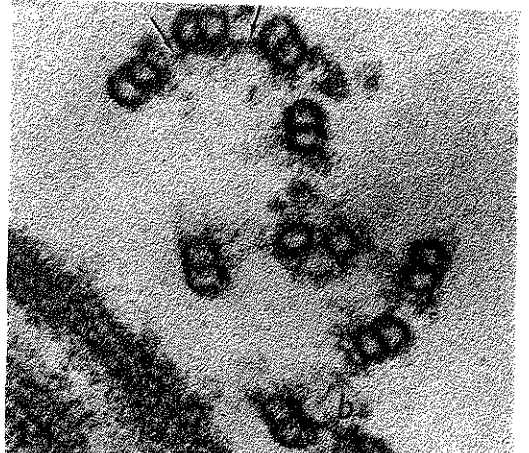
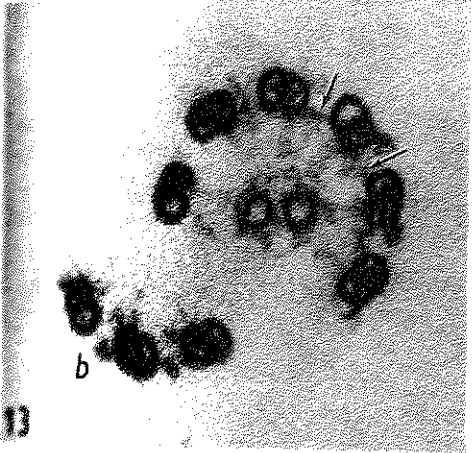
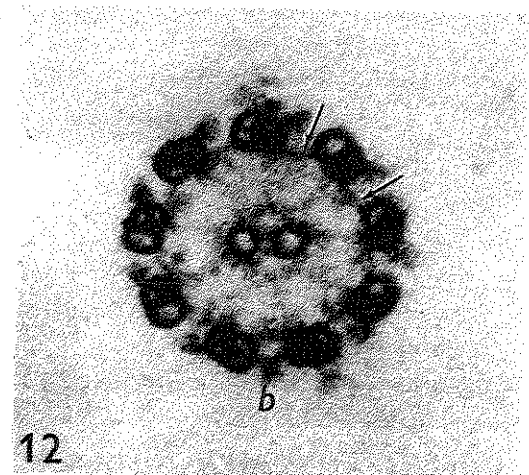
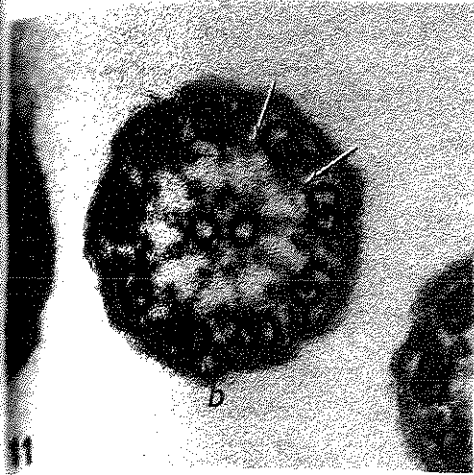
Fig. 15. Longitudinal section in the region of 3 adjacent doublets of an *in situ* cilium. Dynein arms are visible along 2 of the doublets (arrows). Several interdoublet links (lines) can be seen connecting adjacent *a* and *b* subfibres. The links repeat at 86 nm along the subfibres and are positioned at an angle of about 45° from the perpendicular, indicating that some sliding displacement has occurred between the 2 doublets. $\times 160000$.

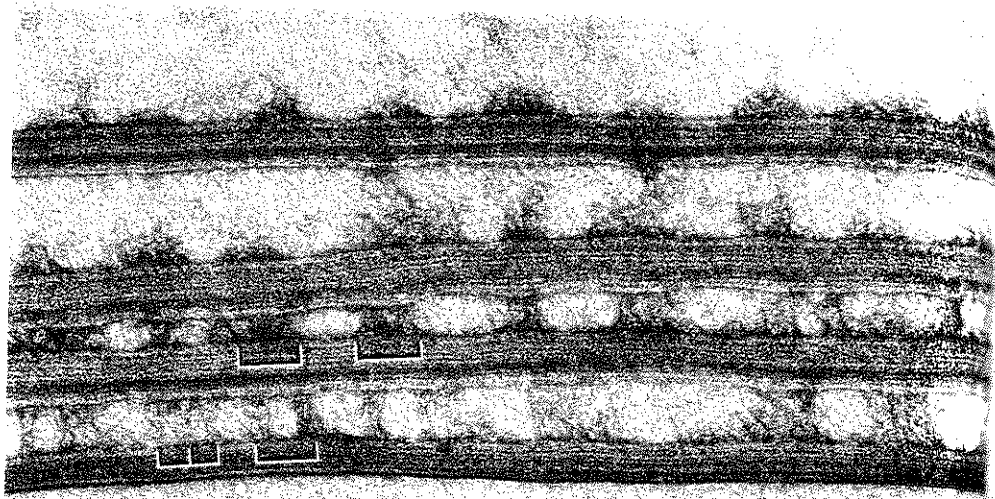


Interdoublet links (arrows) connect the inner dynein arms. The direction of the doublets 5-6 bridge (b) located in the

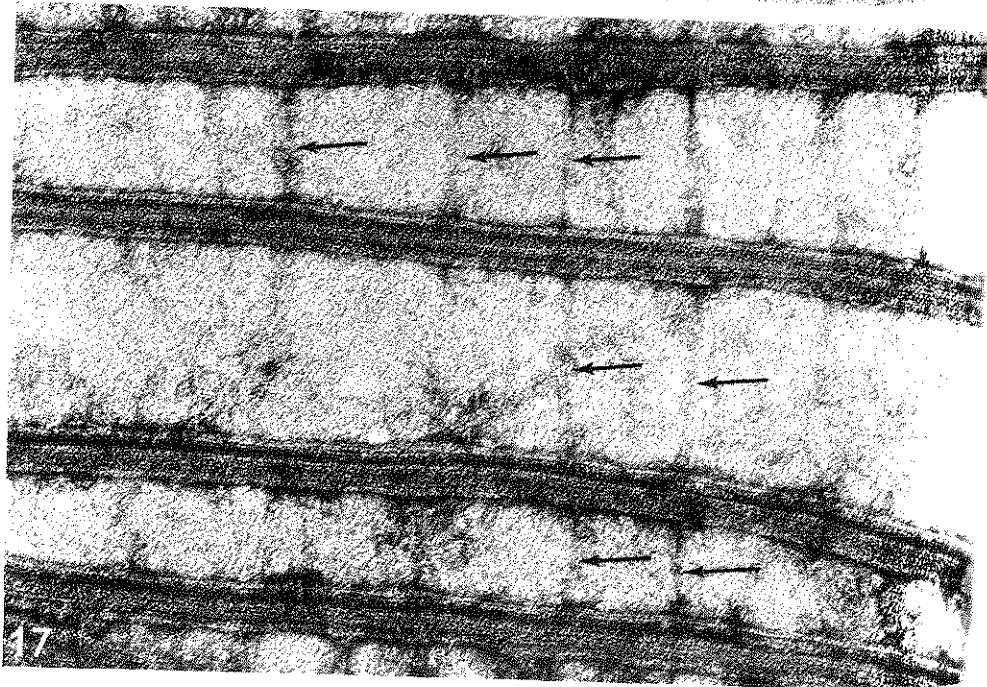
in varying degrees of disassociation, particularly clear in Fig. 12. Cilium in Fig. 11.

Adjacent doublets of an *in situ* cilium (arrows). Several interdoublet links connect microtubule bundles. The links repeat at 86 nm, at about 45° from the perpendicular, occurred between the 2 doublets.





16



17

Fig. 16. Uranyl acetate negatively contrasted doublet microtubules. The groups of triplet radial spokes (brackets) repeat at 86 nm along the doublet and often clumped together so that individual spokes are not resolved. The spoke groups appear to be holding the doublets together on the carbon support film although this is an artifactual condition that occurred during collapse and staining of the axonemal

Fig. 17. Several doublets from a single cilium which show thin connexions (arrows) with a 50–100 nm repeat between the doublets. The links appear to have stretched considerably since doublet separation is about 150 nm. Spoke groups have apparently been solubilized from these 4 doublets (subfibre A is at the top of each) but were visible in the remaining doublets similar to Fig. 16.

A LOCALIZED ZONE OF PROLIFERATION IN THE AXONEMAL DILEPTIN CYCLES OF *GYMNODIMORPHUS*

J. KINK
*Nencki Inst.
 Cell Biology*

SUMMARY

In the ciliate *Dileptus*, growth intensifies, increasing the growth of the cytotosomal field. The growth includes the stimulation of the growth of the cytotosomal apparatus with the proliferation of the cytotosomal field. The proliferation of the cytotosomal field is observed in those regions of somatic ciliature and somatic ciliature. The mode of proliferation of the cytotosomal field is found in a localized position in relation to the proliferation of the cytotosomal field.

INTRODUCTION

In ciliates thus far studied (Lattar, 1967; Lattar, 1972) the cell can form and grow on a localized zone of the cell with a rapid rate of growth. The excysted cell of the ciliate is characterized by a narrow zone of the cytotosomal parts of the cytotosomal apparatus and ingested material. In these excysted cells there are two possible modes of proliferation: an enlargement